# Solution–Liquid–Solid Growth of Semiconductor Quantum-Wire Films

**Fudong Wang,* Virginia L. Wayman, Richard A. Loomis, and William E. Buhro***

Department of Chemistry and Center for Materials Innovation, Washington University, St. Louis, Missouri 63130-4899, United States

**ABSTRACT** We report the growth of cadmium-selenide (CdSe) quantum-wire (QW) films on a variety of substrates by the solution–liquid–solid (SLS) method. Our SLS syntheses employ size-controlled, near-monodisperse bismuth (Bi) nanoparticles (NPs) as the catalysts for QW growth, which offers several advantages over Bi NPs thermally generated from thin Bi films, including mean QW diameter control, narrow diameter distributions, small diameters in the quantum-confinement regime, and control of the QW density on the substrates. The Bi NPs are deposited on the substrates via drop casting of a Bi-NP solution and subsequently annealed in a reducing atmosphere, a key step to ensure firm attachment of the Bi NPs onto the substrates and maintenance of their catalytic activity for the QW-film growth. The QW growth density is proportional to the Bi-NP coating density, which is determined by the concentration of the Bi-NP deposition solution. Lower concentrations are used for small Bi NPs to reduce their high tendency for agglomeration and to achieve control over mean QW diameter and to produce narrow diameter distributions. Spectroscopic evidence of quantum confinement is provided. Related films of InP, InAs, and PbSe QWs are also described.

**KEYWORDS:** solution–liquid–solid growth · semiconductor · quantum wire · film · substrate · bismuth

Semiconductor-nanowire arrays on substrates have drawn increasing interest for their potential applications in field emission,[1,2] lasing,[3] solar cells,[4] batteries,[5] and piezoelectrics.[6] Among the various approaches, vapor-phase methods have been widely used for the growth of high-quality and high-density nanowire arrays of various compositions.[1−3,5−10] Solution-phase methods, including the SLS approach,[12,13] provide promising alternatives and have been recently applied to the synthesis of semiconductor nanowire arrays or films.[4,14−18] The mild, low-temperature synthetic conditions and potentially scalable production enabled by solution-based methods allow a wider range of substrates and promise a more cost-effective fabrication relative to the vapor-phase approaches.

Adaptations of the original colloidal SLS method[12,13,19] have been developed for the growth of semiconductor-nanowire films. Park and co-workers described the fabrication of SLS-derived CdSe, CdS, and CdSe/CdS heterojunction nanowire films on Si substrates.[14] Subsequently Sung and co-workers reported SLS-derived CdS nanowire films on conductive glass.[15] More recently, Dorn, Bawendi, and co-workers have grown CdSe[16] and InP[17] nanowire films on Pt electrodes using an electrically controlled SLS synthesis. However, for the reasons outlined below, in none of these cases was purposeful control of nanowire diameter or growth density on the substrate achieved. Furthermore, the nanowire films did not exhibit quantum-confinement effects because the nanowire diameters were generally large. These nanowires were not QWs, that is, nanowires having diameters smaller than approximately twice the bulk exciton Bohr radius.

The previous SLS film syntheses employed thin Bi films deposited on the growth substrates to generate the Bicatalyst NPs.[14−17] As shown in Scheme 1a, the films were heated near the bulk melting point of Bi (271 °C) to promote their thermal breakup into NPs having various spontaneously formed sizes and spacings. Because the NPs generated by this method tend to be large and have broad diameter distributions, the nanowires grown from them have large mean diameters and broad diameter distributions. We proposed that the deposition and attachment of premade, near-monodisperse Bi NPs on growth substrates (Scheme 1b) would provide control of nanowire diameter and density, and allow access to small mean diameters within the quantum-confinement regime. The success of that strategy is demonstrated in this work.

## RESULTS AND DISCUSSION

Our synthesis of CdSe QW films followed the methods that we developed previously for the SLS growth of colloidal CdSe QWs from Bi NPs.[19,20] The procedure is depicted in Scheme 2 (see Methods for more details). A Si (111) wafer (~50 mm$^2$) was cleaned in a series of solvents and then etched in buffered hydrofluoric acid to remove organic residues and surface oxide, respectively (Scheme 2a). A drop of purified Bi NP

* Address correspondence to buhro@wustl.edu, fwang@wustl.edu.

Received for review April 11, 2011 and accepted April 28, 2011.

**Published online April 28, 2011**
**10.1021/nn201336z**

solution in toluene was immediately applied onto the Si wafer (Scheme 2b), and the Bi-NP deposited Si wafer was then placed in a quartz tube into which purified tri-*n*-octylphosphine oxide (TOPO, ca. 1 g) was added to the upstream side (Scheme 2c). After purging with a mixture of $H_2$ (10%) and Ar (90%) for 1 h, the substrate was annealed in a tube furnace at a desired temperature in the same gas mixture for 20 min. As the substrate was subsequently cooled, it was tethered (in air) to a Ti wire and loaded into a reaction tube containing the premade Cd-precursor stock solution (Scheme 2d). The reaction tube was then heated to a desired temperature into which the selenium (Se) stock solution was injected to initiate QW growth.

Annealing is essential to firmly attach the Bi NPs onto the substrates. Without annealing or after annealing at insufficient temperatures (<200 °C), the deposited Bi NPs were partially or completely desorbed from the substrates into the solution. NP desorption resulted in no wire growth or a low wire growth density on the substrates (by SEM), and the growth of colloidal wires in the solution (by TEM).

The annealing step did not produce an apparent morphology change in the Bi NPs, even at the high temperature end of 300−350 °C range examined (Figures 1, S1, and S2, Supporting Information). Annealing did induce a small increase in the mean diameter of about 6% (Figures 1 and S1). Elemental Bi engages in a eutectic transformation with Si at a temperature close to the melting point of Bi (271 °C), but with a negligible Si solubility in Bi even at 800 °C (Figure S3, Supporting Information).[21] Dissolution of such a small amount of Si into the Bi NPs at 300−350 °C thus had a negligible effect on the diameter increase. The diameter increase was apparently due to the flattening of the Bi NPs as a

**Scheme 1. SLS Growth of Semiconductor Nanowire Films Employing (a) Thin Bi Films and (b) near-Monodisperse Bi NPs**

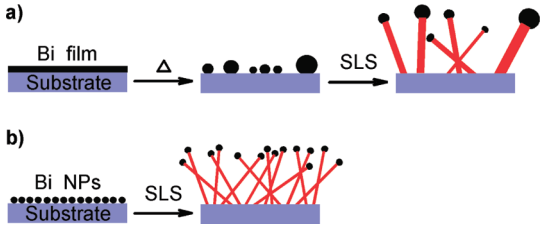


**Scheme 2. Synthetic Procedure for QW Films: (a) Substrate Cleaning, (b) Bi-NP Deposition on the Substrate, (c) Bi-NP Annealing, and (d) Synthesis of QW Films[a]**

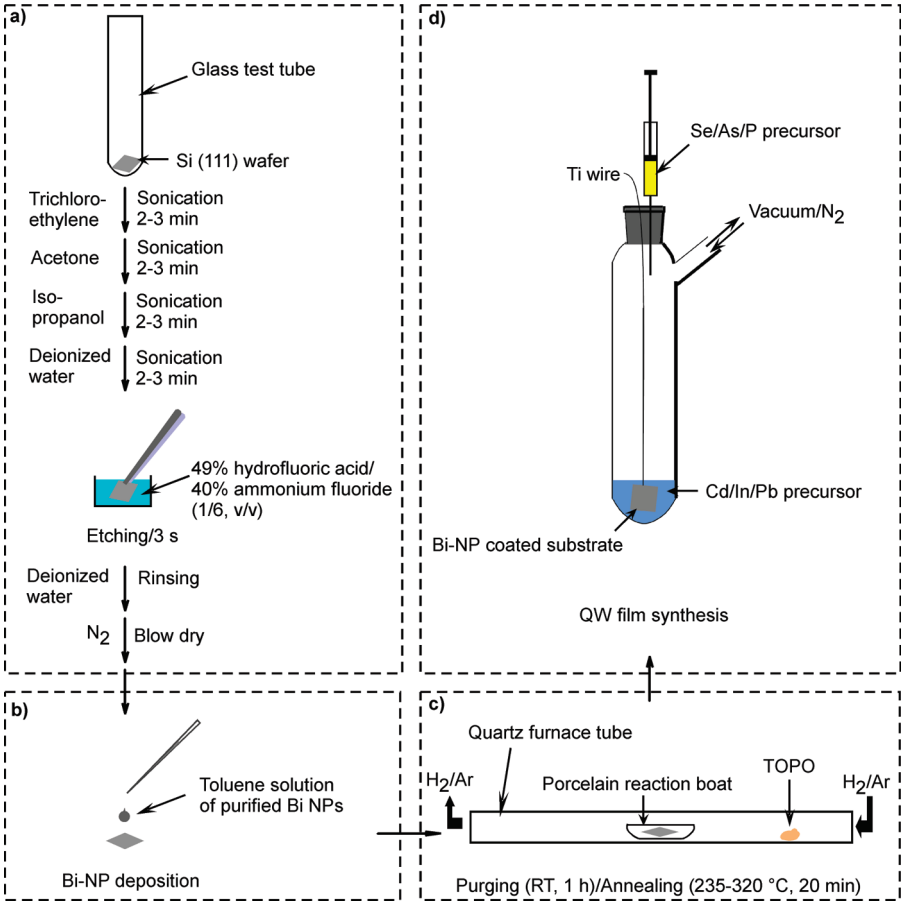


[a] Refer to the Methods for details and other substrates used.

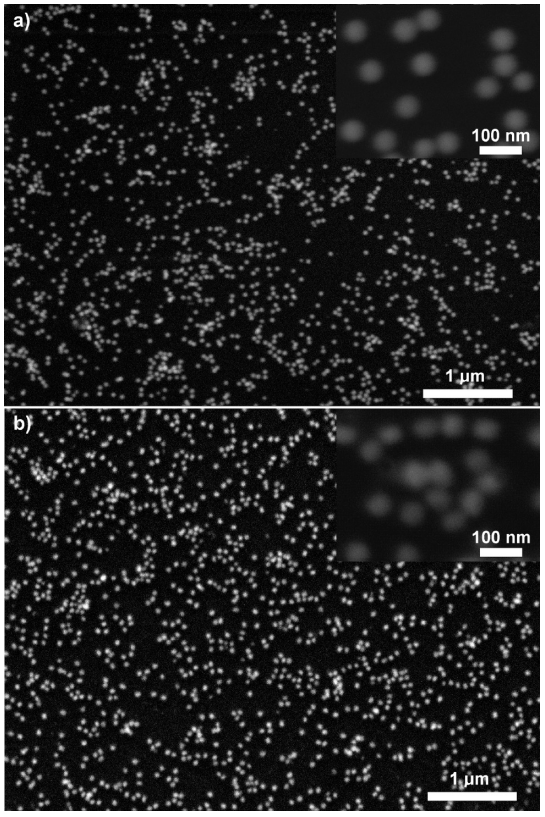


**Figure 1. Representative SEM images of Bi NPs on Si (111) wafer (a) before and (b) after annealing at 320 °C for 20 min in the presence of $H_2$ (10%) and Ar (90%). (Insets) Corresponding high-resolution SEM images. The concentration of Bi-NP deposition solution was 1.6 $\mu$mol Bi atoms mL$^{-1}$ in toluene. The diameter (*d*) of the Bi NPs employed was 54.5 nm ± 5% (measured from TEM images). The *d* values (measured from the SEM images) were 53.2 nm ± 8% (before annealing) and 56.4 nm ± 9% (after annealing), respectively. Because of insufficient SEM resolution, such before and after size measurements could not be made for small (i.e., *d* = 4.8 nm) Bi NPs.**

result of their wetting of the Si surface. This flattening was extreme after annealing at 610 °C where the Bi NP mean diameter increased by ~40% (Figure S4, Supporting Information). No agglomerations of the Bi NPs on the substrates are evident after the annealing step, even at high deposition densities (up to a very high deposition concentration of 2.4 $\mu$mol Bi atoms mL$^{-1}$ in toluene, Figures 1 and S2).

The purification of the Bi NPs in air (see Methods) and/or air exposure of the NPs after the annealing step resulted in a loss of their catalytic activity. Bi NPs annealed under $N_2$ failed to catalyze SLS growth, and were recovered intact upon the substrate after such attempts (Figure S5, Supporting Information). Consequently, a reducing $H_2$/Ar atmosphere was employed during annealing to prevent adventitious oxidation of the NPs. The TOPO employed in the annealing procedure condensed a thin protective coating on the NPs as the substrate cooled, allowing the annealed substrates to be transferred in air. Control SLS experiments employing a $H_2$/Ar atmosphere but omitting TOPO gave

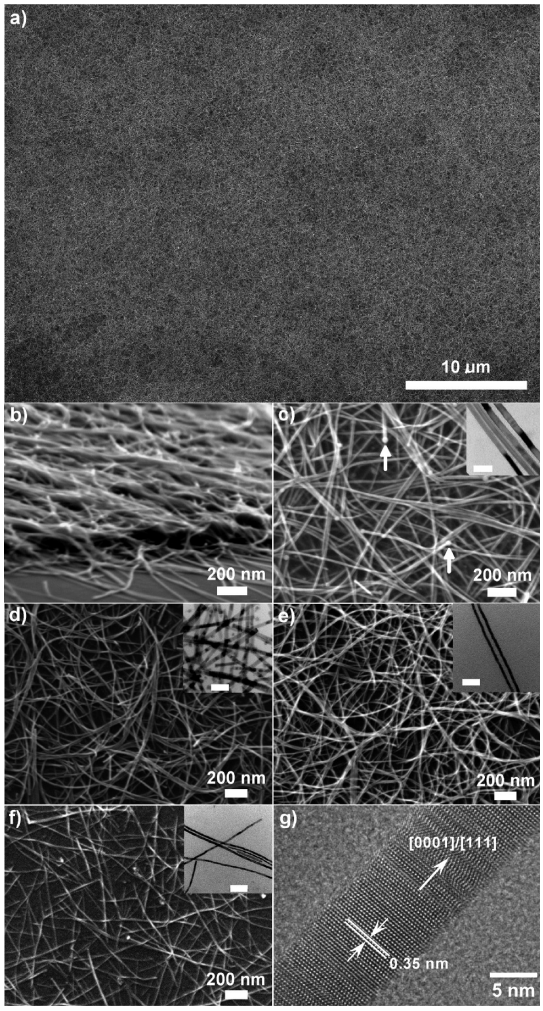


**Figure 2. Representative SEM and TEM (insets) images of CdSe QWs of various diameters, *d*, grown on Si (111). (a–c) *d* = (16.0 ± 2.0) nm (±13%), (d) *d* = (12.0 ± 1.9) nm (±16%), (e) *d* = (7.4 ± 1.3) nm (±18%), and (f) *d* = (5.1 ± 0.9) nm (±18%) grown from 29.4 nm, 16.1 nm, 8.8 nm, and 4.8 nm Bi NPs, respectively. (a) Low-resolution SEM image, showing the QW coverage on the substrate. (b) Forty-five degree tilted-view SEM image. Arrows in (c) indicate the Bi tips at the ends of wires. (c–f, insets) Corresponding TEM images with scale bars of 50 nm. (g) Lattice-resolved HRTEM image of a 10-nm-diameter CdSe QW viewed in the zinc blende (ZB) [011] or wurtzite (WZ) [2$\bar{1}\bar{1}$0] zone normal to the growth axis of ZB [111] and WZ [0001]. The measured *d* spacings for ZB (111) and WZ (0001) planes were 0.35 nm, consistent with the bulk value of 0.35 nm for CdSe.[19]**

little wire growth and primarily intact, inactive NPs adhering to the substrate (Figure S6, Supporting Information). Consequently, both the reducing atmosphere and TOPO protective coating were essential to fixing the Bi NPs upon the growth substrates and preserving their catalytic activity for wire growth.

A representative region of a CdSe QW film obtained from the synthetic procedure described above is shown in Figure 2a. The CdSe wires covered almost the entire (7 mm × 7 mm) substrate surface with a film thickness of ~200 nm, although thickness variations were observed (Figure 2b). For this specific sample, the wire growth time was 1 min and the concentration of the Bi-NP

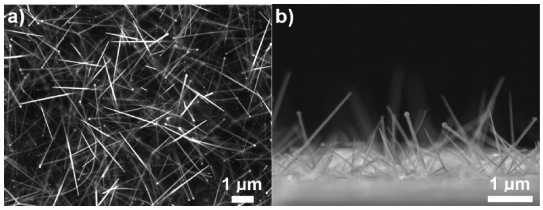


**Figure 3. SEM images of CdSe QW films on a Si (111) substrate at an early stage (after 15 s of growth): (a) top view and (b) cross-sectional view.**

deposition solution (to control the Bi-NP coating density; see below) was 0.4 $\mu$mol Bi atoms mL$^{-1}$. The film thickness did not increase with reaction time. As shown in Figure S7a (Supporting Information), a similar film thickness was achieved with a shorter (0.5 min) wire growth time. However, the film thickness increased from ~100 nm to ~1 $\mu$m with increasing Bi NP coating densities as the concentration of Bi NP-toluene solutions was varied from 0.16 to 1.6 $\mu$mol Bi atoms mL$^{-1}$ (Figures 2b and S7b,c, Supporting Information).

The growth of CdSe QWs followed the SLS mechanism, as evidenced by the presence of Bi tips at the ends of wires (Figures 2c and S8, Supporting Information). Many wires formed bundles (aggregates of wires aligned in parallel) as indicated in the SEM images (Figure 2c–f, and see Figure S9, Supporting Information, for corresponding lower- and higher-resolution SEM images). The wire mean diameters measured from TEM images (Figure 2c–f insets) were varied over the range of 5–16 nm with the standard deviations in the diameter distributions of less than 20% of the mean diameter (Figure S10, Supporting Information). These diameter distributions were only slightly broader than those previously obtained in the colloidal SLS syntheses (standard deviations of 10–14% of mean diameter),[19] and indicated diameter near monodispersity. The lengths of the wires were typically several micrometers. The wire compositions were confirmed to be CdSe by EDX (Figure S11, Supporting Information) and HRTEM (Figure 2g), where the nanowires showed zinc blende and wurtzite alternations, consistent with previous observations.[19,22]

The diameter of wires was primarily controlled by the size of the Bi NPs employed. However, the coating density of Bi NPs on the substrates, determined by the concentration of the Bi NP-toluene solutions (Figure S2, Supporting Information), was very influential to the diameter control achieved. Better diameter control was obtained with lower Bi-NP coating densities, especially for the smaller Bi NPs. The concentration of Bi NP–toluene solutions was varied from 0.13 to 0.4 $\mu$mol Bi atoms mL$^{-1}$ toluene, with the lowest concentration used for small Bi NPs (Figure 2). Small (i.e., 4.8 nm diameter) Bi NPs at a higher concentration (i.e., 1.6 $\mu$mol Bi atoms mL$^{-1}$ toluene) resulted in the growth of thicker nanowires having broad diameter distributions as a result of Bi NP agglomeration (Figure S12, Supporting Information).

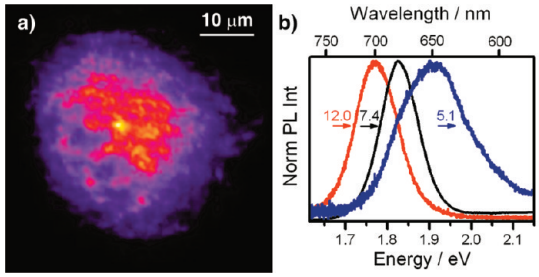


**Figure 4. Room-temperature (RT) photoluminescence (PL) of CdSe QW films. (a) A representative PL microscopy image for the 12-nm-diameter CdSe QW film (Figure 2d). (b) Representative PL spectra (with normalized intensity) for the CdSe QW films shown in Figure 2d–f with diameters of 12.0, 7.4, and 5.1 nm. The corresponding PL peaks (FWHMs) are 1.774 (0.123), 1.829 (0.108), and 1.913 eV (0.198 eV), respectively. The bulk CdSe band gap (RT) is 1.75 eV.**

Control experiments, as mentioned above, showed no agglomerations of the Bi NPs on the substrates after the annealing step, even at high deposition densities (i.e., 2.4 $\mu$mol Bi atoms mL$^{-1}$, Figure S2b, Supporting Information). The results suggested that the agglomeration of Bi NPs may have occurred after the wire growth was initiated. As thinner wires have greater bending flexibility, the Bi tips on thinner wires at high wire growth densities might have a greater tendency to collide and coalesce, thus resulting in the growth of significantly thicker wires and broadened diameter distributions. The coalescence of catalyst NPs on growing wires should produce branched structures, and such wire branching is evident in TEM images (Figure S12b, Supporting Information).

Epitaxial wire growth was not achieved on Si (111). As shown in Figures 2 and S7–9 (Supporting Information), the long wires lie roughly parallel to the surface of the substrate, obscuring the crystallographic relationship between the wires and substrate. Shorter wires imaged at earlier growth stages were not aligned parallel to the substrate surface (Figure 3). However, a statistical analysis of their pointing angles established that they were randomly oriented, thus excluding epitaxial growth (Figure S13, Supporting Information). The failure of epitaxial growth was likely due to the large lattice mismatch (12%) between CdSe and Si (111).[23] However, vertically oriented nanowires of InAs having a similar lattice mismatch (12%)[23] with Si have been grown epitaxially on Si (111).[9–11] In addition, vertically oriented CdSe nanowires were reported to grow epitaxially on mica (001), although there is an even larger (17%) lattice mismatch.[24] Efforts to achieve vertical wire growth by the SLS method are currently under way.

The wire diameters in the smallest-diameter CdSe nanowire films obtained here suggested that such films should exhibit quantum-confinement effects (the exciton Bohr radius for bulk CdSe = 5.4 nm). Indeed, the films exhibited diameter-dependent photoluminescence (PL) as a result of quantum confinement in the radial QW dimension (Figure 4). The

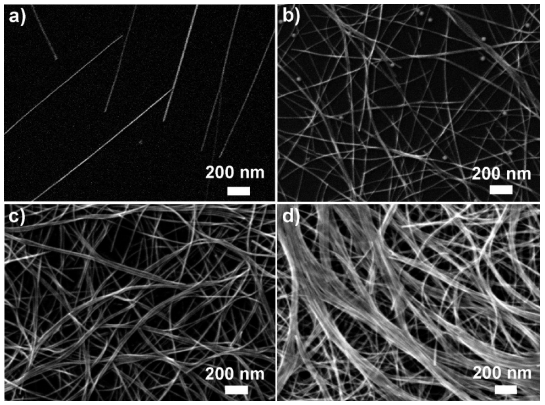


**Figure 5. Representative top-view SEM images of CdSe QWs of various densities grown from Si (111) using Bi NP concentration of (a) 0.02, (b) 0.08, (c) 0.4, and (d) 1.6 $\mu$mol Bi atoms mL$^{-1}$. The diameters of the Bi NPs are (a−c) 29.4 nm and (d) 8.8 nm, respectively.**

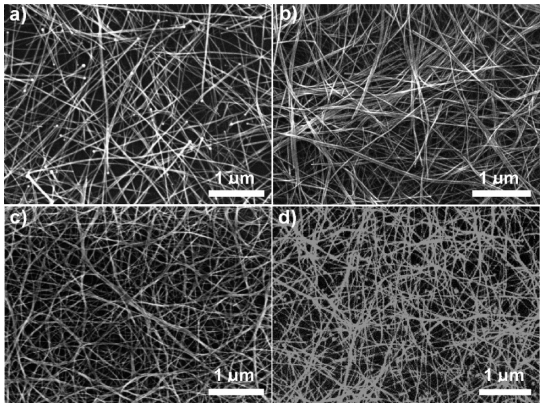


**Figure 6. Representative top-view SEM images of CdSe QWs grown from various substrates: (a) Si (100), (b) Indium−tin-oxide (ITO)-coated glass slide, (c) glass cover slide, and (d) polyimide sheet. The diameters of the Bi NPs used were (a) 29.4 nm, (b) 8.8 nm, and (c,d) 16.1 nm, respectively.**

diameter dependence of the PL peak positions agreed with that we previously reported for the colloidal CdSe QWs,[19] although the full widths at half-maximum (fwhm) of 108−190 meV were larger, as compared to 75−103 meV,[19] due to the broader diameter distributions for the wires grown on substrates (16−18%) than those for the colloidal CdSe nanowires (10−14%).[19] The PL intensity varied as the PL was acquired at different locations, due to the variation in film thickness discussed above, although no apparent variations in the breadths or shapes of the emission profiles were observed. Wires grown from densely coated 4.8 nm Bi NPs exhibited red-shifts in PL peak position and broad fwhm, which is consistent with the TEM observations above that these wires had larger diameters and broad diameter distributions as a result of Bi NP agglomeration (Figure S12, Supporting Information).

We demonstrated control over the wire growth densities by varying the coating density of Bi NPs on the substrates. As shown in Figure 5, the density of wires was varied from 0.4 to 40.2 wires $\mu$m$^{-2}$ as the

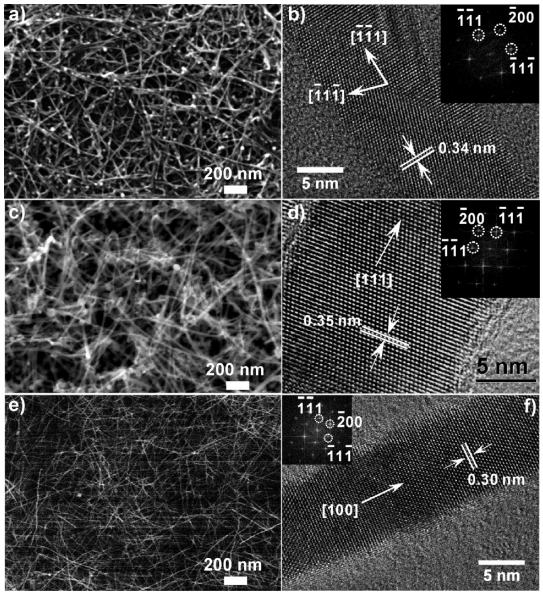


**Figure 7. Representative SEM (left column) and HRTEM (right column) images of (a,b) InP, (c,d) InAs, and (e,f) PbSe QWs grown on an ITO-coated glass slide, Si (111) wafer, and polyimide sheet, respectively. The *d* values of the QWs (and Bi NPs used) were (a,b) 12.3 nm ±15% (29.4 nm), (c,d) ∼18 nm (39.7 nm), and (e,f) ∼10 nm (8.8 nm), respectively. The QWs in (b,d,f) were viewed in the [011] zone. The measured *d* spacings were (b) 0.34 nm, (d) 0.35 nm, and (f) 0.30 nm, consistent with the bulk values of 0.3388 nm for InP (111) (ICDD-PDF No. 00−032−0452), 0.3498 nm for InAs (111) (ICDD-PDF No. 00−015−0869), and 0.3062 nm for PbSe (200) (ICDD-PDF No. 00−006−0354), respectively.**

concentration of the Bi-NP deposition solution was varied from 0.02 to 1.6 $\mu$mol Bi atoms mL$^{-1}$. A greater tendency to bundling was observed for higher-density wire films (Figure 5c,d), where the diameters of the wires were still under control (Figure S14, Supporting Information). Because we could not count all the wires underneath the top layers and in the bundles for higher-density wire films (Figure 5d), the value 40.2 wires $\mu$m$^{-2}$ is an underestimate. We expect that the low-density wires are ideal for the study of single-wire spectroscopy,[25−27] whereas the high-density wires may be suitable for applications in solar cells.[4,15]

As an additional study, we investigated whether QWs could be grown on substrates other than Si (111). QW growth was attempted on Si (100), indium−tin-oxide (ITO)-coated glass, glass microscopy cover slides, and polyimide sheets, and their representative SEM images are shown in Figure 6. The QWs possess comparable qualities with the QWs grown on Si (111) in terms of control over QW diameter, length, and growth density. Since glass and plastics are considerably cheaper than silicon, QWs grown on glass and plastics may thus provide additional advantages for potential applications.

Preliminary results also established that this method can be extended to the growth of other semiconductor

QW films on substrates, including InP,[28] InAs,[29] and PbSe (Figures 7, S15, and S16, Supporting Information).[30] Due to their narrow direct bulk band gaps (1.35 eV for InP, 0.35 eV for InAs, and 0.28 eV for PbSe at 300 K), these QWs have wide light absorption windows, making them potentially more advantageous for photovoltaic applications.

## CONCLUSION

In summary, we have demonstrated that the SLS method can be successfully applied to the growth of semiconductor QW films on substrates with substantial control over QW diameters, diameter distributions, growth density, and compositions. The method holds great promise for the integration of semiconductor QWs into electronic and photonic devices at low cost and low temperatures (<320 °C), as the wire growth temperatures (220−320 °C) are compatible with various substrates and technologies. The challenge of achieving densely packed, vertically oriented QW arrays is currently under study.

## METHODS

**Materials.** Si (111) wafer (phosphorus-doped), Si (100) wafer (boron-doped), ITO-coated glass slides (ITO thickness = 150−300 Å) were purchased from Aldrich. Glass cover slides and polyimide sheets (0.076 nm thick) were purchased from Fisher and CS Hyde, respectively. Bismuth (Bi) NP stock solutions (0.04 mmol Bi atoms $g^{-1}$ solution)[19,31] and di-*n*-octylphosphinic acid (DOPA)[20,32] were synthesized using previously reported procedures. Tri-*n*-octylphosphine oxide (TOPO) was purified from the technical grade TOPO (~90%, Aldrich) using a previously reported procedure.[20] Tri-*n*-octylphosphine (TOP, 90%, Aldrich), oleic acid (OA, 90%, Aldrich), selenium shot (Se, 99.999%, amorphous, Alfa Aesar), cadmium oxide (CdO, 99.99%, Aldrich), and *n*-tetradecylphosphonic acid (TDPA, high grade ~99%, PCI Synthesis) were used as received. The saturated TOPSe stock solution was prepared using a previously reported procedure.[20] The cadmium (Cd)-precursor stock solution was prepared[20] by heating a mixture of CdO (5 mg, 0.039 mmol), OA (70 mg, 0.25 mmol), TDPA (6 mg, 0.022 mmol), DOPA (8 mg, 0.028 mmol), and purified TOPO (5 g, 12.9 mmol) in a 50-mL Schlenk reaction tube at 320 °C to achieve a clear, nearly colorless solution (~50 min) and subsequently cooling it to room temperature for later use. Other reagents were used as received.

**Substrate Preparation and Bi NP Deposition.** A 50-$mm^2$ substrate cut from a Si wafer was cleaned for 2−3 min in each solvent in the order of trichloroethylene, acetone, isopropanol, and deionized (DI) water in an ultrasonic bath, and then etched for 3 s in a buffered hydrofluoric-acid (HF) solution (6:1 (v:v) of 40 wt % aqueous ammonium fluoride solution to 49 wt % aqueous HF solution). The substrate was rinsed with DI water for 1 min and dried under an $N_2$ stream for 1 min for immediate use in subsequent Bi-NP deposition. ITO-coated glass slides, glass cover slides, or polyimide sheets were cleaned in acetone for 10 s in an ultrasonic bath prior to use. The Bi NPs were isolated in the ambient atmosphere from the stock solution (10−60 mg, 0.4−2.4 $\mu$mol Bi atoms) by adding toluene (ca. 1 mL) and methanol (ca. 4 mL) to the stock solution, followed by centrifugation of the stock solution and decanting of the supernatant. The precipitate containing Bi NPs was redispersed in toluene (1−20 mL) to obtain Bi NP solutions (0.02−2.4 $\mu$mol Bi atoms $mL^{-1}$ toluene) for later Bi-NP deposition on substrates. The Bi-NP concentrations were estimated based on the assumptions that all Bi precursors used were converted to Bi NPs and all Bi NPs were recovered during isolation. The substrate was placed horizontally on a CVD porcelain reaction boat and a drop of the Bi-NP solution was applied and spread out spontaneously on the surface of the substrate (~50 $mm^2$). The reaction boat was then inserted into the center of a quartz furnace tube and purified TOPO (ca. 1 g) was added (~10 cm away from the boat) to the upstream side of the tube. The tube was placed in a tube furnace and purged in a flow of $H_2$ (10%) and Ar (90%) with a flow rate of 20−40 $cm^3$ standard temperature and pressure $min^{-1}$ for the entire annealing process. After the system was purged at room temperature for 1 h, the substrate was heated to the desired annealing temperature within 20 min and annealed for 20 min. The annealing temperature was 235, 260, 280, and 320 °C for 4.8, 8.8, 16.1, and 29.4 nm Bi NPs, respectively. The substrate was cooled to near room temperature and tethered to a Ti wire for immediate use in the subsequent growth of QW film.

**Synthesis of CdSe QW Films.** The synthesis was adapted from a procedure reported previously.[20] In a typical preparation of 7.4 nm diameter (±18%) CdSe QW film, the (solid) Cd-precursor stock solution (1 g) was loaded into a 50-mL Schlenk reaction tube and degassed under vacuum (0.01−0.1 Torr) for 15 min and backfilled with $N_2$ (dry, oxygen-free gas if not otherwise specified). The Ti-wire tethered substrate (coated with 8.8 nm Bi NPs using a concentration of 0.4 $\mu$mol Bi atoms $mL^{-1}$ toluene) was quickly inserted into the tube and the tube was degassed for 5 min and backfilled with $N_2$. The degassing and $N_2$ backfilling were repeated two additional times. TOPSe (125 mg, 0.28 mmol), and TOP (25 mg, 0.067 mmol) were combined in a vial, which was septum capped. The mixture of TOPSe and TOP was then loaded into a syringe. The Schlenk tube was heated to 262 °C in a salt bath and the substrate was immersed in the melted Cd-precursor stock solution, and after 2 min the mixture of TOPSe and TOP was quickly injected into the tube (the amount injected was ~100 mg). No stirring was required. An orange solution color resulted in about 1 min and the wire growth was terminated by lifting the substrate (using the Ti wire) out of the reaction mixture and withdrawing the tube from the bath. The substrate was cleaned in the ambient atmosphere by applying a toluene stream onto the surface for subsequent SEM and photoluminescence characterizations. For TEM characterizations, the QW films were sonicated in toluene (~1 mL) for 10 min and carbon-coated copper grids were dipped in the toluene solutions and then immediately taken out to evaporate the solvent.

**SEM, TEM, and Spectroscopic Analyses.** SEM images of the QW films were collected using a JEOL 7001LVF FE-SEM. TEM images and EDX spectroscopy of the QWs were collected using a JEOL 2000 FX microscope with an acceleration voltage of 200 kV. The diameter statistics for the QWs were measured by the commercial software Image Pro Progress (version 4.5) at the 2× zoom from 200−500 wires in TEM images taken at a magnification of 500 000× , expressed as the statistical mean diameter ± one standard deviation. High-resolution TEM (HRTEM) was carried out on a JEOL JEM-2100F TEM at 200 kV. Photoluminescence (PL) microscopy images and spectra were collected at room temperature using epi-fluorescence with a spectrophotometer mounted onto an inverted microscope, with a Plan Apo 40x, 0.95NA objective. CdSe QW films were excited using a 488 nm cw laser, with a power density of approximately 100 W $cm^{-2}$. An exposure time of 100 ms and 1 s were used to acquire PL images and spectra, respectively.

*Acknowledgment.* This work was supported by NSF (CHE-1012898 for W. Buhro and DMR-0906966 for R. Loomis).

*Supporting Information Available:* SEM images of Bi NPs on substrates before and after annealing, Bi–Si phase diagram, SEM images of CdSe wires grown from Bi NPs annealed in the absence of $H_2$ or without TOPO, SEM images of Bi NPs having various coating densities, additional SEM images of CdSe QW films, diameter-distribution histograms for CdSe QWs, and EDX spectra of CdSe, InP, InAs, and PbSe QWs. This material is available free of charge via the Internet at http://pubs.acs.org.

## REFERENCES AND NOTES


1. Pan, Z. W.; Lai, H. L.; Au, F. C. K.; Duan, X. F.; Zhou, W. Y.; Shi, W. S.; Wang, N.; Lee, C. S.; Wong, N. B.; Lee, S. T.; et al. Oriented Silicon Carbide Nanowires: Synthesis and Field Emission Properties. *Adv. Mater.* **2000**, *12*, 1186–1190.
2. Lee, C. J.; Lee, T. J.; Lyu, S. C.; Zhang, Y.; Ruh, H.; Lee, H. J. Field Emission from Well-Aligned Zinc Oxide Nanowires Grown at Low Temperature. *Appl. Phys. Lett.* **2002**, *81*, 3648–3649.
3. Huang, M. H.; Mao, S.; Feick, H.; Yan, H.; Wu, Y.; Kind, H.; Weber, E.; Russo, R.; Yang, P. Room-Temperature Ultraviolet Nanowire Nanolasers. *Science* **2001**, *292*, 1897–1899.
4. Law, M.; Greene, L. E.; Johnson, J. C.; Saykally, R.; Yang, P. Nanowire Dye-Sensitized Solar Cells. *Nat. Mater.* **2005**, *4*, 455–459.
5. Chan, C. K.; Peng, H. L.; Liu, G.; McIlwrath, K.; Zhang, X. F.; Huggins, R. A.; Cui, Y. High-Performance Lithium Battery Anodes Using Silicon Nanowires. *Nat. Nanotech.* **2007**, *3*, 31–35.
6. Wang, Z. L.; Song, J. H. Piezoelectric Nanogenerators Based on Zinc Oxide Nanowire Arrays. *Science* **2006**, *312*, 242–246.
7. Hochbaum, A. I.; Fan, R.; He, R.; Yang, P. Controlled Growth of Si Nanowire Arrays for Device Integration. *Nano Lett.* **2005**, *5*, 457–460.
8. Kuykendall, T.; Pauzauskie, P. J.; Zhang, Y.; Goldberger, J.; Sirbuly, D.; Denlinger, J.; Yang, P. Crystallographic Alignment of High-Density Gallium Nitride Nanowire Arrays. *Nat. Mater.* **2004**, *3*, 524–528.
9. Mårtensson, T.; Wagner, J. B.; Hilner, E.; Mikkelsen, A.; Thelander, C.; Stangl, J.; Ohlsson, B. J.; Gustafsson, A.; Lundgren, E.; Samuelson, L.; et al. Epitaxial Growth of Indium Arsenide Nanowires on Silicon Using Nucleation Templates Formed by Self-Assembled Organic Coatings. *Adv. Mater.* **2007**, *19*, 1801–1806.
10. Tomioka, K.; Motohisa, J.; Hara, S.; Fukui, T. Control of InAs Nanowire Growth Directions on Si. *Nano Lett.* **2008**, *8*, 3475–3480.
11. Wei, W.; Bao, X.-Y.; Soci, C.; Ding, Y.; Wang, Z.-L.; Wang, D. Direct Heteroepitaxy of Vertical InAs Nanowires on Si Substrates for Broad Band Photovoltaics and Photodetection. *Nano Lett.* **2009**, *9*, 2926–2934.
12. Trentler, T. J.; Hichman, K. M.; Goel, S. C.; Viano, A. M.; Gibbons, P. C.; Buhro, W. E. Solution–Liquid–Solid Growth of Crystalline III–V Semiconductors: an Analogy to Vapor–Liquid–Solid Growth. *Science* **1995**, *270*, 1791–1794.
13. Wang, F.; Dong, A.; Sun, J.; Tang, R.; Yu, H.; Buhro, W. E. Solution–Liquid–Solid Growth of Semiconductor Nanowires. *Inorg. Chem.* **2006**, *45*, 7511–7521.
14. Ouyang, L.; Maher, K. N.; Yu, C. L.; McCarty, J.; Park, H. Catalyst-Assisted Solution–Liquid–Solid Synthesis of CdS/CdSe Nanorod Heterostructures. *J. Am. Chem. Soc.* **2007**, *129*, 133–138.
15. Kwak, W.-C.; Kim, T. G.; Lee, W.; Han, S.-H.; Sung, Y.-M. Template-Free Liquid-Phase Synthesis of High-Density CdS Nanowire Arrays on Conductive Glass. *J. Phys. Chem. C* **2009**, *113*, 1615–1619.
16. Dorn, A.; Wong, C. R.; Bawendi, M. G. Electrically Controlled Catalytic Nanowire Growth from Solution. *Adv. Mater.* **2009**, *21*, 3479–3482.
17. Dorn, A.; Allen, P. M.; Bawendi, M. G. Electrically Controlling and Monitoring InP Nanowire Growth from Solution. *ACS Nano* **2009**, *3*, 3260–3265.
18. Greene, L. E.; Law, M.; Tan, D. H.; Montano, M.; Goldberger, J.; Somorjai, G.; Yang, P. General Route to Vertical ZnO Nanowire Arrays Using Textured ZnO Seeds. *Nano Lett.* **2005**, *5*, 1231–1236.
19. Wang, F.; Buhro, W. E. An Easy Shortcut Synthesis of Size-Controlled Bismuth Nanoparticles, and Their Use in the SLS Growth of High-Quality Colloidal Cadmium Selenide Quantum Wires. *Small* **2010**, *6*, 573–581.
20. Wang, F.; Tang, R.; Kao, J. L.-F.; Dingman, S. D.; Buhro, W. E. Spectroscopic Identification of Tri-*n*-octylphosphine Oxide (TOPO) Impurities and Elucidation of Their Roles in Cadmium Selenide Quantum-Wire Growth. *J. Am. Chem. Soc.* **2009**, *131*, 4983–4996.
21. Massalski, T. B. *Binary Alloy Phase Diagrams*, Vol. 1; American Society for Metals: Metals Park, OH, 1986; pp 538–539.
22. Grebinski, J. W.; Hull, K. L.; Zhang, J.; Kosel, T. H.; Kuno, M. Solution-Based Straight and Branched CdSe Nanowires. *Chem. Mater.* **2004**, *16*, 5260–5272.
23. Adachi, S. *Handbook of Physical Properties of Semiconductors*; Springer: New York, 2004; pp 46, 312, 574.
24. Utama, M. I. B.; Peng, Z.; Chen, R.; Peng, B.; Xu, X.; Dong, Y.; Wong, L. M.; Wang, S.; Sun, H.; Xiong, Q. Vertically Aligned Cadmium Chalcogenide Nanowire Arrays on Muscovite Mica: A Demonstration of Epitaxial Growth Strategy. *Nano Lett.* **2011**, 10.1021/nl1034495.
25. Glennon, J. J.; Tang, R.; Buhro, W. E.; Loomis, R. A. Synchronous Photoluminescence Intermittency (Blinking) along Whole Semiconductor Quantum Wires. *Nano Lett.* **2007**, *7*, 3290–3295.
26. Glennon, J. J.; Buhro, W. E.; Loomis, R. A. Simple Surface-Trap-Filling Model for Photoluminescence Blinking Spanning Entire CdSe Quantum Wires. *J. Phys. Chem. C* **2008**, *112*, 4813–4817.
27. Glennon, J. J.; Tang, R.; Buhro, W. E.; Loomis, R. A.; Bussian, D. A.; Htoon, H.; Klimov, V. I. Exciton Localization and Migration in Individual CdSe Quantum Wires at Low Temperatures. *Phys. Rev. B* **2009**, *80*, 081303.
28. Wang, F.; Yu, H.; Li, J.; Hang, Q.; Zemlyanov, D.; Gibbons, P. C.; Wang, L.-W.; Janes, D. B.; Buhro, W. E. Spectroscopic Properties of Colloidal Indium Phosphide Quantum Wires. *J. Am. Chem. Soc.* **2007**, *129*, 14327–14335.
29. Wang, F.; Yu, H.; Jeong, S.; Pietryga, J. M.; Hollingsworth, J. A.; Gibbons, P. C.; Buhro, W. E. The Scaling of the Effective Band Gaps in Indium Arsenide Quantum Dots and Wires. *ACS. Nano* **2008**, *2*, 1903–1913.
30. Sun, J. High-Quality Colloidal II-VI and IV-VI Semiconductor Nanowires: Diameter-Controlled Synthesis, Quantum-Confinement-Effect Studies, and Electronic Structure. PhD Thesis, Washington University (U.S.A.), 2008.
31. Wang, F.; Tang, R.; Yu, H.; Gibbons, P. C.; Buhro, W. E. Size- and Shape-Controlled Synthesis of Bismuth Nanoparticles. *Chem. Mater.* **2008**, *20*, 3656–3662.
32. Wang, F.; Tang, R.; Buhro, W. E. The Trouble with TOPO; Identification of Adventitious Impurities Beneficial to the Growth of Cadmium Selenide Quantum Dots, Rods, and Wires. *Nano Lett.* **2008**, *8*, 3521–3524.